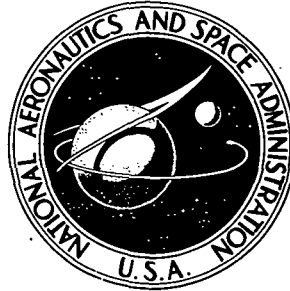


NASA TECHNICAL NOTE



N73-18082  
NASA TN D-7198

NASA TN D-7198

CASE FILE  
COPY

EXPERIMENTAL TEST RESULTS OF  
A GENERALIZED-PARAMETER FUEL CONTROL

*by Peter G. Batterton and Harold Gold*

*Lewis Research Center*

*Cleveland, Ohio 44135*

|   |   |  |                             |
|---|---|--|-----------------------------|
| 1. Report No.<br><b>NASA TN D-7198</b>  | 2. Government Accession No.                                 | 3. Recipient's Catalog No.                                     |                             |
| 4. Title and Subtitle<br><b>EXPERIMENTAL TEST RESULTS OF A GENERALIZED-<br/>PARAMETER FUEL CONTROL</b>  |   | 5. Report Date<br><b>March 1973</b>                            |                             |
|   |   | 6. Performing Organization Code                                |                             |
| 7. Author(s)<br><b>Peter G. Batterton and Harold Gold</b>   |   | 8. Performing Organization Report No.<br><b>E-7254</b>         |                             |
|   |   | 10. Work Unit No.<br><b>501-24</b>                             |                             |
| 9. Performing Organization Name and Address<br><b>Lewis Research Center<br/>National Aeronautics and Space Administration<br/>Cleveland, Ohio 44135</b>   |   | 11. Contract or Grant No.                                      |                             |
|   |   | 13. Type of Report and Period Covered<br><b>Technical Note</b> |                             |
| 12. Sponsoring Agency Name and Address<br><b>National Aeronautics and Space Administration<br/>Washington, D.C. 20546</b>   |   | 14. Sponsoring Agency Code                                     |                             |
|   |   | 15. Supplementary Notes  |                             |
| 16. Abstract<br><p>Considerable interest has been generated recently in low-cost jet propulsion systems. One of the more complicated components of jet engines is the fuel control. Results of an effort to develop a simpler hydromechanical fuel control are presented. This prototype fuel control was installed on a J85-GE-13 jet engine. Results show that the fuel control provided satisfactory engine performance at sea-level static conditions over its normal nonafterburning operating range, including startup. Results of both bench and engine tests are presented; the difficulties encountered are described.</p> |   |  |                             |
| 17. Key Words (Suggested by Author(s))<br><b>Turbojet engine controls<br/>Hydromechanical controls<br/>Propulsion fuel controls</b>   |   | 18. Distribution Statement<br><b>Unclassified - unlimited</b>  |                             |
| 19. Security Classif. (of this report)<br><b>Unclassified</b>   | 20. Security Classif. (of this page)<br><b>Unclassified</b> | 21. No. of Pages<br><b>28</b>                                  | 22. Price*<br><b>\$3.00</b> |

\* For sale by the National Technical Information Service, Springfield, Virginia 22151

# EXPERIMENTAL TEST RESULTS OF A GENERALIZED-PARAMETER

## FUEL CONTROL

by Peter G. Batterton and Harold Gold

Lewis Research Center

### SUMMARY

Considerable interest has been generated recently in low-cost jet propulsion systems. One of the more complicated components of jet engines is the fuel control. As a result, a simpler hydromechanical fuel control was developed. This fuel control is based on the use of linear schedules for acceleration and deceleration fuel flow limits. These schedules are linear when plotted in terms of generalized corrected engine parameters.

A prototype control based on this scheme was designed and built. This control was sized for operation of a J85-GE-13 jet engine in the nonafterburning mode. A test bench was used to calibrate and check out the fuel control before installation on the engine. Results of these bench tests and the difficulties encountered are presented. Results of engine tests are included; they show that the fuel control provided satisfactory performance of the engine at sea-level static conditions over its normal nonafterburning operating range. Only sea-level tests were performed. Successful engine startup was also demonstrated and an example is given. The fuel control mechanization and its operation are described in detail.

### INTRODUCTION

Recent interest in low-cost jet propulsion systems has led to an investigation of propulsion systems and propulsion system components (ref. 1). The fuel control is one of the more costly propulsion system components associated with turbojet engines. Its primary purpose is to control fuel flow in such a manner as to regulate engine rotor speed at a value demanded by the power lever input position. Also when the power lever is advanced to a higher setting, the fuel control must supply additional fuel to the engine to increase speed. However, this increase must be limited to values that do not cause

compressor surge or excessive turbine temperatures. Likewise, if the power level is changed to a lower setting, the fuel control must reduce the amount of fuel supplied to the engine, but not so much as to cause the combustor to blow out.

Reference 2 analyzes a fuel control that is based on a potentially low-cost hydro-mechanical mechanism. The control utilizes acceleration and deceleration limits that are based on generalized parameters, corrected fuel flow over corrected speed and compressor pressure ratio (fig. 1). The results of that study indicate that a considerable reduction in control complexity could be achieved when the acceleration and deceleration fuel-flow limits are described as linear functions of the generalized parameters. The mathematical analysis of the hydromechanical control with predicted engine performance data is presented in reference 2.

The work presented in this report was conducted to test a prototype hydromechanical fuel control based on the design used for the mathematical analysis of reference 2. These tests would uncover any difficulties in using this potentially low-cost hydromechanical design. The fuel control was sized for testing on a J85-GE-13 engine. The physical mechanization of the control simulated in reference 2 is described. Also the operation of the fuel control is discussed. Bench tests were performed before the fuel control was installed on the engine for the engine tests.

During the bench tests, it was determined that the orifice flow areas for the deceleration fuel-flow limit were too large. As a "quick fix," one of the deceleration fuel-flow limit areas was sealed off. This, however, would allow the deceleration limit to vary with altitude, rather than as shown in figure 1. Therefore, only sea-level bench and engine tests were performed. Results of both the bench and engine sea-level tests are presented.

## SYMBOLS

|                      |  |
|----------------------|--|
| $A_{\text{eff}}$     | effective area of $A_1$ to $A_6$ , $\text{cm}^2$             |
| $A_1, \dots, A_6$    | fuel control orifice areas, $\text{cm}^2$                    |
| $C_1, \dots, C_{12}$ | constants (units as required)                                |
| $c$                  | orifice discharge coefficient                                |
| $d$                  | control-gear-pump flow gain, $0.737 \text{ (kg/hr)/percent}$ |
| $N$                  | engine speed, percent of maximum rated                       |
| $P_a$                | main-pump discharge pressure, $\text{N/cm}^2$                |
| $P'_a$               | control-gear-pump discharge pressure, $\text{N/cm}^2$        |

|  |  |
|--|--|
| $P_b$  | control output pressure, $N/cm^2$            |
| $P_c$  | governor output pressure, $N/cm^2$           |
| $P_{STD}$  | standard-day pressure, $10.12 N/cm^2$        |
| $P_2$  | compressor face pressure, $N/cm^2$           |
| $P_3$  | compressor exit pressure, $N/cm^2$           |
| $T_{STD}$  | standard-day temperature, $288 K$            |
| $T_2$  | compressor face temperature, $K$             |
| $\dot{W}_1, \dots, \dot{W}_6, \dot{W}_{in}, \dot{W}_T$ | control fuel flows, $kg/hr$                  |
| $\delta$   | pressure correction, $P_2/P_{STD}$           |
| $\theta$   | temperature correction, $T_2/T_{STD}$        |
| $\rho$   | fuel density, $0.806 \times 10^{-3} kg/cm^3$ |

## OPERATION AND PHYSICAL DESCRIPTION

The function of this fuel control is to meter fuel flow to regulate engine rotor speed as demanded by the power lever. When the power lever is changed, the fuel control must also limit fuel flow to appropriate values until new equilibrium is reached. These fuel flow limits are based on generalized parameters, corrected fuel flow over corrected speed and compressor pressure ratio. It was determined that a potentially low-cost hydromechanical control could be designed when these limits are defined as linear functions of the generalized parameters, as shown in figure 1. The acceleration limit is defined as

$$\frac{\dot{W}_T / \delta \sqrt{\theta}}{N / \sqrt{\theta}} = C_{11} \frac{P_3}{P_2} + C_{12} \quad (1)$$

And the deceleration limit is defined as

$$\frac{\dot{W}_T / \delta \sqrt{\theta}}{N / \sqrt{\theta}} = C_{10} \frac{P_3}{P_2} \quad (2)$$

This section of this report describes the mechanical operation of the fuel control and how the schedules shown in figure 1 are produced.

## Operation

A simplified schematic of the fuel control is shown in figure 2. The schedules of equations (1) and (2) require fuel flow to be proportional to engine speed. A small control gear pump driven by engine speed is used to generate the reference fuel flow. This fuel flow passes through the reference orifice  $A_1$  to provide a reference pressure drop  $P'_a - P_b$ . The upstream pressure  $P'_a$  is used to provide the reference pressure to the bypass pressure regulator. The bypass pressure regulator is used to regulate the output pressure of the main fuel pump. In this case, the bypass pressure regulator regulates the output pressure such that the reference pressure drop  $P'_a - P_b$  also appears across the metering orifices.

The main fuel pump supplies all the fuel used by the control and thus by the engine. This fuel flow can vary over a wide range for various engine conditions. Therefore, the capacity of the main fuel pump must be made greater than the maximum delivered by the control to the engine under all operating conditions. The bypass pressure regulator then bypasses all excess fuel not used by the engine.

Orifices  $A_1$ ,  $A_5$ , and  $A_6$  determine the deceleration fuel-flow limit; and orifices  $A_1$ ,  $A_3$ ,  $A_4$ ,  $A_5$ , and  $A_6$  determine the acceleration fuel-flow limit. The governor orifice,  $A_2$ , controls the flow through  $A_3$  and  $A_4$  and thus modulates fuel flow between the two fuel-flow limits.

Zero-gradient pump and bypass pressure regulator operation. - The zero-gradient pump principle is employed to obtain a fuel flow which is proportional to engine speed and independent of operating pressures. This is achieved by driving the control gear pump with engine speed. The fuel-flow output of the control gear pump passes through a reference orifice to the output of the fuel control. The pressure drop across the reference orifice  $A_1$  is then proportional to  $N^2$ . The upstream pressure of the reference orifice is  $P'_a$ , which also acts on one side of the bypass pressure regulator. Since there are no other forces acting on the bypass regulator except the output pressure of the high-pressure pump  $P_a$ , the bypass regulator regulates  $P_a$  at a value equal to  $P'_a$ . Since  $P'_a$  is also the input pressure to the control gear pump, there is no pressure rise across it and, hence, it is called a "zero gradient" pump.

The pressure drop that appears across the metering orifice section of the fuel control is denoted by  $P_a - P_b$ . Since the flow through the reference orifice is proportional to speed and  $P'_a$  is equal to  $P'_a$ , fuel flow through the metering orifices will also be proportional to  $N$ . The fuel flow through the zero-gradient pump is equal to the flow gain of the pump multiplied by the pump speed (which is proportional to engine speed). Thus,

$$\dot{W}_1 = d \times N \quad (3)$$

The leakage terms have been neglected, because there is zero pressure gradient across the pump. The fuel flow through the reference orifice is

$$\dot{W}_1 = cA_1 \sqrt{2\rho} \sqrt{P'_a - P_b} \quad (4)$$

Solving these two equations for  $\sqrt{P'_a - P_b}$  in terms of  $N$  and noting that  $P_a = P'_a$ , we obtain

$$\sqrt{P_a - P_b} = \frac{d \times N}{cA_1 \sqrt{2\rho}} \quad (5)$$

Since  $P_a - P_b$  is the pressure drop across the metering orifices of the fuel control, the fuel flow out of the fuel control will be

$$\dot{W}_T = cA_{\text{eff}} \sqrt{2\rho} \sqrt{P_a - P_b} \quad (6)$$

where  $A_{\text{eff}}$  equals effective area at  $A_1$  to  $A_6$ . Substituting equations (5) into (6),

$$\dot{W}_T = \frac{d \times N \times A_{\text{eff}}}{A_1} \quad (7)$$

Thus, the total fuel output of the control will be proportional to  $N$  and independent of control operating pressure.

**Metering orifices.** - Orifices  $A_2$  to  $A_6$  in figure 2 are used to produce the fuel-flow output of the control. The governor orifice  $A_2$  modulates between open and closed. It is fully closed for the deceleration limit and fully open for the acceleration limit. Its opening is controlled by the governor spool position, which is a function of  $P_a - P_b$  (engine speed) and the power lever. The remaining orifices ( $A_3$  to  $A_6$ ) are positioned by compressor inlet pressure  $P_2$  and compressor discharge pressure  $P_3$ . These are the only other sensed engine variables.

Figure 3 is a simplified cross-sectional view of the generalized-parameter fuel control. The  $P_2$  and  $P_3 - P_2$  spools are positioned by a force balance of these engine pressures and the spring bias for each spool, respectively. The  $P_2$  spool is primarily an altitude compensator, where areas  $A_4$  and  $A_6$  are linear functions of  $P_2$ . The  $P_3 - P_2$  spool compensates for the compressor pressure rise, where areas  $A_3$  and  $A_5$  are linear functions of  $P_3 - P_2$ .

Variable reference orifice operation. - The reference orifice  $A_1$  shown in figure 3 is not strictly a fixed-area orifice as represented in the preceding section. Under normal engine operation, however, the piston is bottomed out, causing  $A_1$  to be at its maximum value. At engine speeds below idle this is not true. The reason is to provide an enrichment of the fuel supplied the engine during startup. This enrichment is required, since engine efficiency drops off at low speed and the acceleration fuel-flow limit as defined in figure 1 is too low. When engine speed is low enough,  $P'_a - P_b$  is too low to overcome the spring force on the variable reference orifice piston (fig. 3). When this occurs, the orifice area becomes smaller than normal. This has the effect of providing a  $P'_a - P_b$  that is greater than the normal value described by equation (5). Thus, additional fuel is provided to the engine. As engine speed increases,  $P'_a - P_b$  increases and eventually completely overcomes the spring force on the piston. When this occurs, the reference orifice will be at its design area and the fuel control will be operating normally. The spring force and rate are chosen so that the reference orifice reaches its maximum area before the engine reaches idle speed.

Governing operation. - The purpose of the governor is to control fuel flow to the engine for steady-state or near steady-state operation. As mentioned in the preceding section,  $A_2$  is the governor orifice. Its fully open and fully closed points determine the acceleration and deceleration limit conditions. The governor spool is positioned by a force balance of the  $P_a - P_b$  pressure (engine speed) and the bias springs. A power lever speed command change is entered into this system by changing the precompression on the bias spring at the  $P_b$  end of the spool. The governor orifice  $A_2$  will then open (or close, depending on the direction of the commanded change) until a  $P_a - P_b$  is achieved which starts to close (or open)  $A_2$ . The final  $A_2$  must provide sufficient flow for steady-state engine operation again. For the prototype control tests, the  $A_2$  orifice had a nonlinear characteristic, which tended to reduce the governor gain when engine gain was high (low corrected fuel flows).

Deceleration operation. - For a power lever decrease, the spring force on the  $P_b$  end of the governor spool is decreased. The governor spool thus moves to the left, decreasing  $A_2$ . For a large power lever decrease,  $A_2$  will completely close, cutting off all flow to  $A_3$  and  $A_4$ . Thus, the fuel flow supplied to the engine will be proportional to  $A_1 + A_5 + A_6$ . These areas determine the deceleration fuel-flow limit for the fuel control. From appendix B of reference 2, we can write the equation for the minimum fuel flow:

$$\dot{W}_T = \frac{d \times N}{A_1} (A_1 + A_5 + A_6) \quad (8)$$

$$\dot{W}_T = \frac{d \times N}{A_1} [A_1 + C_4 + C_5 P_2 + C_6 (P_3 - P_2)] \quad (9)$$

The  $C$ 's are functions of the spool bias setting, the spring rates, and the orifice widths. By designing  $(d \times C_6)/A_1$  to equal  $C_{10}/P_{STD}$ ,  $C_4$  to equal  $-A_1$ , and  $C_5$  to equal  $C_6$ , equation (9) can be rearranged into the following form:

$$\dot{W}_T = \frac{N}{P_{STD}} C_{10} P_3 \quad (10)$$

Equation (10) can easily be written in the corrected parameter form by dividing both sides by  $P_2/P_{STD}$  (ref. 2, appendix C).

$$\frac{\dot{W}_T / \delta \sqrt{\theta}}{N / \sqrt{\theta}} = C_{10} \frac{P_3}{P_2} \quad (2)$$

This is the deceleration limit shown in figure 1. Then as engine speed decreases,  $P_a - P_b$  decreases and  $A_2$  will open when engine speed becomes low enough. Governing operation is thus obtained.

Acceleration operation. - Likewise, for a power lever increase, the spring force acting on the  $P_b$  end of the governor spool is increased. Orifice  $A_2$  opens and increases fuel flow to the engine through orifices  $A_3$  and  $A_4$ . For a large power lever advance,  $A_2$  will reach a maximum area which is much greater than  $A_3 + A_4$ . Thus, the total fuel flow from the control will be proportional to  $A_1 + A_3 + A_4 + A_5 + A_6$ . This area determines the acceleration fuel-flow limit. Again, from appendix B of reference 2, we can write the equation for the maximum fuel flow:

$$\dot{W}_T = \frac{d \times N}{A_1} (A_1 + A_3 + A_4 + A_5 + A_6) \quad (11)$$

$$\dot{W}_T = \frac{d \times N}{A_1} [A_1 + C_1 + C_2 P_2 + C_3 (P_3 - P_2) + C_4 + C_5 P_2 + C_6 (P_3 - P_2)] \quad (12)$$

By designing  $C_1$  to equal zero,  $d(C_3 + C_6)/A_1$  to equal  $C_{11}/P_{STD}$ , and  $d(C_2 - C_3)/A_1$  to equal  $C_{12}/P_{STD}$  ( $C_4$ ,  $C_5$ , and  $C_6$  were defined by the deceleration limit), equation (12) can be rearranged into the following form:

$$\dot{W}_T = \frac{N}{P_{STD}} (C_{11}P_3 + C_{12}P_2) \quad (13)$$

Equation (13) can easily be expressed in the corrected-parameter form again dividing both sides by  $P_2/P_{STD}$  (ref. 2, appendix C):

$$\frac{\dot{W}_T/\delta\sqrt{\theta}}{N/\sqrt{\theta}} = C_{11} \frac{P_3}{P_2} + C_{12} \quad (1)$$

This is the acceleration limit shown in figure 1. Then as engine speed increases,  $P_a - P_b$  increases and eventually overcomes the additional force from the power lever on the  $P_b$  end of the governor spool. Orifice  $A_2$  will then decrease, cutting back on the fuel supplied to the engine.

Elimination of  $A_6$  orifice. - The elimination of the  $A_6$  orifice was found to permit a lowering of the deceleration fuel-flow limit as required during the bench testing of the control. This, however, introduced an altitude effect into the deceleration fuel flow limit. This altitude effect is tolerable. With  $A_6$  eliminated, equation (9) becomes

$$\dot{W}_T = \frac{d \times N}{A_1} [A_1 + C_6(P_3 - P_2)] \quad (14)$$

With  $(d \times C_6)/A_1$  equal to  $C_{10}/P_{STD}$  equation (14) becomes

$$\dot{W}_T = (d \times N) + (d \times N) \frac{C_{10}}{P_{STD}} (P_3 - P_2) \quad (15)$$

Dividing both sides by  $P_2/P_{STD}$  yields

$$\frac{\dot{W}_T/\delta\sqrt{\theta}}{N/\sqrt{\theta}} = C_{10} \frac{P_3}{P_2} + \frac{d \times P_{STD}}{P_2} - C_{10} \quad (16)$$

The terms  $(d \times P_{STD})/P_2$  and  $C_{10}$  are the effect of orifice  $A_6$ . When the pump flow gain ( $d = 0.737$  (kg/hr)/percent) was used, the deceleration limit was found to increase by 1.363 (kg/hr)/percent as  $P_2$  changed from 10.0 N/cm<sup>2</sup> to 3.5 N/cm<sup>2</sup>.

This altitude effect could also occur on the acceleration limit. However, because

$A_4$  and  $A_6$  are controlled by the same pressure ( $P_2$ ), altitude insensitivity of the acceleration limit can be retained even after the elimination of  $A_6$  if  $C_1$  is set equal to  $-A_1$ ,  $d(C_3 + C_6)/A_1$  is set equal to  $C_{11}/P_{STD}$ , and if  $(d \times C_2)/A_1$  is set equal to  $(C_{11} + C_{12})/P_{STD}$ .

Fuel cutoff valve operation. - Engine fuel-flow initiation and cutoff are provided by the fuel cutoff valve. Whenever the valve is closed, no fuel flow will be supplied to the control (and thus to the engine). Also,  $P'_a$  will drop below the output pressure of the high-pressure pump. Thus, the bypass pressure regulator will bypass all fuel back to the high-pressure pump inlet, effectively unloading the pump.

## Physical Description

Since the fuel control was designed to be installed on a J85-GE-13 engine, it was decided to use the boost and high-pressure pumps already on the engine. This also provided a convenient place to install the fuel control on the engine. The required fuel ports are on the pumps, as well as a gear from which engine speed (power to drive the zero-gradient pump) could be obtained. Several other interesting features of the design which are not shown in figure 3 are discussed here in detail. Figure 4 shows several of the control components and gives an indication of the physical configuration of the components and their sizes relative to each other.

Spools and sleeves. - Three large bores were made through the aluminum control body for the three spools, as well as for the cross passages for fuel and air lines. Then sleeves were inserted into the bores. The sleeves were made of 440F stainless steel hardened to a Rockwell hardness  $R_c$  of 44 to 48. The spools were also made of 440F stainless steel but hardened an  $R_c$  of 51 to 55. By using this technique, it is possible to hold the required dimensional tolerances for the metering orifices. Figure 5 is a detailed sketch showing the  $P_3 - P_2$  spool-sleeve combination which is typical of all three. Sleeves were used for only the small-diameter portion of all three spools. The dimensional tolerance of a spool in a sleeve is 5 to 15 micrometers diametral clearance. It was felt that with this clearance tolerance, fuel leakage into the pressure sensing lines would not be a problem. To prevent side forces from being generated on the spools by the bias springs, the ends of the spools were rounded. Mating surfaces were then attached to the bias springs.

$P_3 - P_2$  spool. - Using sleeves in the control body requires that considerable clearance be provided at the  $P_3 - P_2$  sensing end of that spool. This clearance is to allow for the unequal compression of the O-ring seals between the sleeve and the control body. To avoid air leakage from  $P_3$  to  $P_2$ , a teflon seal was installed on this spool, as shown in figure 5. Air leakage from  $P_3$  to  $P_2$  could cause undesirable pressure

losses in the  $P_3$  and  $P_2$  sensing lines. A similar seal was not required for the  $P_2$  spool, since  $P_2$  is the only pressure acting on that spool.

Variable reference orifice. - Figure 6 is a detailed sketch of the variable reference orifice. The travel of the reference orifice piston is limited. The needle screw can then be adjusted to provide the required reference-pressure-drop-to-speed characteristic, regardless of the leakage around the piston.

Bypass pressure regulator. - Figure 7 is a detailed sketch of the bypass pressure regulator. There are three grooves shown in the side of the regulator piston. The right-most two are to minimize "hydraulic lock." Control gear pump discharge pressure  $P'_a$  is provided by the control gear pump, and this pressure may be sensitive to leakage. Thus, the left-most groove is vented to  $P_a$ . Since  $P_a$  is approximately equal to  $P'_a$ , leakage from  $P'_a$  to  $P_a$  is minimal. Leakage from  $P_a$  around the piston to the bypass return line is summed with the bypass flow. This leakage results in a corrective shift in the bypass regulator piston, and theoretically no errors result.

Flow forces can produce errors in the output pressure of this type of pressure regulator. To minimize these flow forces, the regulator piston used sharp-edge orifices. The initial design for the bypass regulator used square-edge orifices, which led to a stability problem that is discussed later in the section EXPERIMENTAL RESULTS AND DISCUSSION.

## APPARATUS AND PROCEDURES

### Test Bench Description

Before this fuel control was installed on the J85 engine, it was tested in detail to determine its open-loop operating characteristics. A test bench was thus designed which would permit a full range of operation of the control. Figure 8 shows this test bench.

Since the simplified fuel control uses the standard J85 main fuel boost and high-pressure pumps, these were also bench operated over the range of interest. To supply the required variable speed power to these pumps and the control (as the simulated speed input), a two-speed ac motor connected to a 9:1 variable speed drive were used. A magnetic pickup was used to obtain an accurate measurement of the fuel pump shaft speed of this system.

The panel includes a regulated pressure supply to provide a simulated compressor discharge pressure, a vacuum pump to supply a simulated altitude condition, turbine flowmeters to measure the output flow from the control, and various valves to provide loading to the output of the control. Besides the pressure gages on the panel, pressure

transducers were used to measure the reference orifice pressure drop and the output pressure of the fuel control.

Data for the generalized parameter plots were taken as follows:

(1) Acceleration data were obtained by setting the power lever at maximum and setting control speeds with the variable speed drive, lowest speeds first. Compressor exit pressures corresponding to each speed were applied. The output pressure of the control was adjusted to simulate the actual pressure-flow characteristic of the engine. The output flow was then measured.

(2) Deceleration data were obtained by setting the power lever at minimum. The procedure was the same as for the acceleration data; but the highest speed was used first, then working down.

(3) Governing data were obtained in the same manner as the acceleration data, except the power lever was set in the normal operating range.

(4) The reference orifice pressure drop was measured directly for various speed settings.

(5) The output pressure was varied to determine the control output flow sensitivity. Power lever was set at maximum, and speed was held fixed for each characteristic.

## Engine Description

A General Electric J85-GE-13 afterburning turbojet engine was used for the engine phase of this program. This engine is used for several programs at the Lewis Research Center, where it is located in a sea-level static test stand. Dynamic instrumentation available on the test engine includes engine rotor speed, compressor discharge pressure transducers, turbine discharge thermocouples, compressor variable geometry position, exhaust nozzle position, and a fuel control output flowmeter.

The standard J85-GE-13 comes with a variable-area compressor interstage bleed and variable-angle inlet guide vanes. These are coupled together mechanically and controlled by fuel-powered piston-in-cylinder actuators. Variable compressor geometry control is accomplished in a scheduled fashion by the engine's main fuel control. The variable exhaust nozzle is screwjack actuated with the afterburner fuel control scheduling the area. Both compressor variable geometry and variable exhaust nozzle systems were replaced with electro-hydraulic servosystems. The normal compressor variable geometry schedule was programmed on an analog computer. The exhaust nozzle was programmed on an analog computer as a function of speed for this test. This nozzle schedule closely approximated the standard schedule. To avoid turbine overtemperature and also the complexity of a turbine exit temperature control, the nozzle area was scheduled slightly more open than normal near the engine military-speed rating.

For this test, the J85-GE-13 main fuel control was removed, and the prototype generalized-parameter fuel control was mounted in its place on the engine. Figure 9 shows this installation. The actuator that is visible is the fuel cutoff valve actuator. The power lever actuator is hidden from view on the other side of the control.

## EXPERIMENTAL RESULTS AND DISCUSSION

### Bench Tests

Before operating the fuel control on the engine, it was necessary to test the fuel control over its complete operating range on the bench for calibration. These tests would also determine any problems which might affect engine safety.

Some fuel leakage into the  $P_3$  and  $P_2$  sensing lines did occur. The maximum fuel leakage rate into the  $P_3$  line at the maximum control output pressure was typically 0.5 kg/hr. Fuel leakage into the  $P_2$  line was typically 1.5 kg/hr. These fuel flows could have been permitted to pass into the engine. However, during the engine tests, the  $P_2$  line was not connected to the engine, but rather to a container located in the sea-level test cell.

During the calibration phase of the fuel control tests, it was determined that the desired deceleration fuel-flow limit could not be obtained by adjustment of the spool bias screws. After it was determined that the  $P_2$  spool functioned properly, the deceleration fuel-flow port ( $A_6$ ) on that spool was completely sealed off. This allowed adjustment of the bias screws to obtain the results shown in figure 10. Included for information purposes is the steady-state operation fuel flow for the J85-GE-13. It must be pointed out that, without  $A_6$ , an increase in altitude would increase the deceleration limit above that shown in figure 10. All data presented in this report were taken with  $A_6$  sealed.

It is possible to calculate values for the constants  $C_{10}$ ,  $C_{11}$ , and  $C_{12}$  from figure 10. These values can be compared directly to those of reference 2. The constant  $C_{12}$  is the value of corrected fuel flow over corrected speed for the acceleration limit at  $P_3/P_2 = 0$ , and  $C_{10}$  and  $C_{11}$  are the slopes of the limit lines (see eqs. (1) and (2)). The value of  $C_{12}$  was chosen to be lower than that used in reference 2 for two reasons. First, a value of 3.72 kg/hr produced an acceleration limit higher than provided by the standard J85-GE-13 fuel control. Secondly, lowering the limit line to the level shown in figure 10 permitted it to intersect the steady-state operating line at about 102 percent of rated speed. The bench-test values of the constants  $C_{10}$ ,  $C_{11}$ , and  $C_{12}$  are compared with the analytical values in the following table:

| Constant        | Bench-test value,<br>(kg/hr)/percent | Analytical value, <sup>a</sup><br>(kg/hr)/percent |
|-----------------|--------------------------------------|---|
| C <sub>10</sub> | 0.8                                  | 0.7   |
| C <sub>11</sub> | 1.8                                  | 1.88  |
| C <sub>12</sub> | 3.4                                  | 3.72  |

<sup>a</sup>Ref. 2.

The steady-state operating line in figure 10 begins to sweep up for low  $P_3/P_2$ . This is the low-speed range. The acceleration limit as shown in figure 1 would cross below the steady-state operating line. Thus, starting of the engine would be impossible unless it was driven to a sufficiently high speed. The variable reference orifice was used to provide an increase in  $P_a - P_b$ , and this increase is shown in figure 10 as the negative-slope portion of the acceleration limit at the low  $P_3/P_2$  end of the curve.

As mentioned in the section PHYSICAL DESCRIPTION, the governor orifice  $A_2$  modulates fuel flow between the acceleration and deceleration limits. As the difference between the two limits is reduced, the governor characteristic becomes less steep. Thus, governor characteristics shown in figure 10 are not as steep as those shown in reference 2.

During the initial engine tests, the bypass pressure regulator was changed from the square-edge design to the sharp-edge design that is described in the section PHYSICAL DESCRIPTION. Using this regulator, we observed a further lowering of the acceleration limit with a corresponding flatter governor characteristic. These results are shown in figure 11. This further bears out the flattening of the governor characteristic with the decreased acceleration fuel-flow limit.

As has been mentioned, the reference orifice was made variable to provide fuel enrichment during engine startup. Figure 12 shows  $P'_a - P_b$  as a function of the control speed  $N$ . The action of the variable orifice can be seen easily for  $N$  of less than 50 percent.

The output pressure of the fuel control is a function of the pressure drop across the engine spray nozzles as well as of the burner pressure. Therefore, considerable variation of the fuel control output pressure can be expected during normal engine operation. Figure 13 shows the fuel control output flow-pressure characteristic for four control output flows. The governor was held fixed by setting the power lever at maximum. The increase in fuel flow with increasing output pressure indicates that there are flow forces acting on the bypass pressure regulator. As shown in figure 13, there is approximately a 10 percent increase in the nominal fuel flow as output pressure increases from 138 to 310  $N/cm^2$ . What happens is that as the output pressure increases,  $P'_a$  increases an

equal amount. The bypass pressure regulator bypasses flow from  $P_a$  and also senses  $P_a$ . Thus, as  $P'_a$  increases, the regulator tries to increase  $P_a$  also. However, as  $P_a$  increases, the flow velocity through the bypass regulator increases and the flow forces increase, causing a positive offset in the regulated value of  $P_a$ . During governing operation of the fuel control, the governor will try to offset this effect, since it is positioned by  $P_a - P_b$  rather than by  $P'_a - P_b$ .

## Engine Tests

The initial engine test showed an instability in the governor spool. Stability in the simulation of reference 2 was obtained by simply adding viscous damping until stability was obtained. Unfortunately, the hydromechanical fuel control did not have sufficient viscous friction. The stability problem was solved by installing a 1.6-millimeter-diameter orifice in the governor spool  $P_a$  sensing line. The location of this orifice is shown in figure 3.

Two acceleration traces from engine idle speed are shown in figure 14, the acceleration shown in figure 14(a) is to 95 percent of rated speed, while that shown in figure 14(b) is to 100 percent. Figure 14(a) clearly shows the retarding of fuel flow by the governor as engine speed approaches 95 percent. This effect is not seen on the acceleration trace to 100 percent (fig. 14(b)), since the acceleration fuel-flow limit value is very close to that required by the engine to maintain 100 percent of rated speed.

The data for figure 14 were obtained with a square-edge-orifice bypass pressure regulator. A second instability was observed, however, which could be characterized as a low-frequency limit cycle oscillation (about 1 Hz) of engine speed around the set-point. The cause of this limit cycle oscillation apparently was a flow force acting on the bypass regulator piston and resulting in incorrect bypass regulator operation. The solution to this instability therefore was the incorporation of the sharp-edge bypass regulator piston described in the section PHYSICAL DESCRIPTION. The remaining engine tests were performed with this sharp-edge orifice design.

The final results of the sea-level static engine tests are presented in figures 15 and 16. Engine transients are presented in figure 15, and figure 16 is a typical steady-state point. These figures include the following engine parameters: rotor speed  $N$ , compressor discharge pressure  $P_3$ , exhaust gas temperature (EGT), compressor variable geometry position (VG), variable exhaust nozzle position (VEN), fuel flow  $W_T$ , and power lever angle (PLA).

Engine startup. - Engine startup is accomplished by air motoring the engine to 15 percent. With the PLA at idle setting, the ignitor is started, followed by opening of the fuel cutoff valve. The engine start is shown in figure 15(a). The discontinuity in the

EGT trace is caused by the turning off of the air-start system which affects the EGT thermocouples. The chirp in the fuel-flow trace is electrical noise from the ignitor and occurs whenever the ignitor is turned on.

Engine acceleration. - Figures 15(b) to (d) provide engine acceleration data. Figure 15(b) is a PLA advance of idle to 95 percent of rated speed. This is a cruise condition on a normal J85-GE-13 engine. Careful examination of the fuel-flow trace shows that the governor does actually cut back on fuel as speed approaches 95 percent. This retarding of fuel flow is not as great in figure 15(b) as in figure 14(a) because of the lower acceleration limit. The lower acceleration limit also leads to longer acceleration times, but the values shown in figures 15(b) to (d) are acceptable. The acceleration times could have been improved to the results of figure 14 by further adjustment of the bias screws. The acceleration time in figure 14(a) is approximately 2 seconds, while in figure 15(b) the time is 3 seconds.

Engine deceleration. - Figure 15(e) is a deceleration from 100 percent to idle. Again, careful examination of the fuel-flow trace shows the governor bringing up fuel flow to maintain idle speed.

Steady-state operation. - Figure 16 is a typical trace of the engine parameters with no disturbance to PLA. Speed regulation appears to be better than 1 percent at 90 percent of rated speed. It was this value or better at all normal engine operating points.

## SUMMARY OF RESULTS

A fuel control was designed as a potentially low-cost hydromechanical mechanism. This fuel control utilizes acceleration and deceleration limits that are based on generalized parameters, corrected fuel flow over corrected speed and compressor pressure ratio. Bench tests indicate that the hardware mechanized the desired control schedules at sea-level conditions. The orifice areas of the spools were not perfectly sized to implement these schedules at all altitudes. To accomplish this the orifice areas would have to be recalculated and new spools fabricated. The control was then installed on a J85-GE-13 engine for sea-level static condition tests. The results of those tests show that the fuel control provided satisfactory engine performance over its normal nonafterburning operating range including startup.

Lewis Research Center,  
National Aeronautics and Space Administration,  
Cleveland, Ohio, December 1, 1972,  
501-24.

## REFERENCES

1. Cummings, Robert L.; and Gold, Harold: Low-Cost Engines for Aircraft. Aircraft Propulsion. NASA SP-259, pp. 211-231.
2. Seldner, Kurt; and Gold, Harold: Computer and Engine Performance Study of a Generalized Parameter Fuel Control for Jet Engines. NASA TN D-5871, 1970.

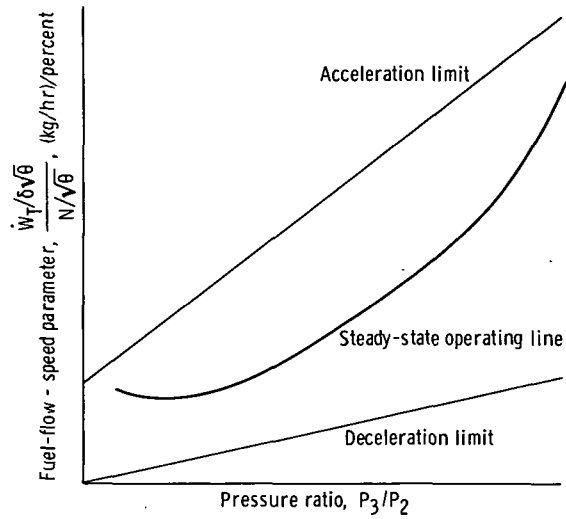


Figure 1. - Corrected parameter map employed in prototype generalized-parameter fuel control.

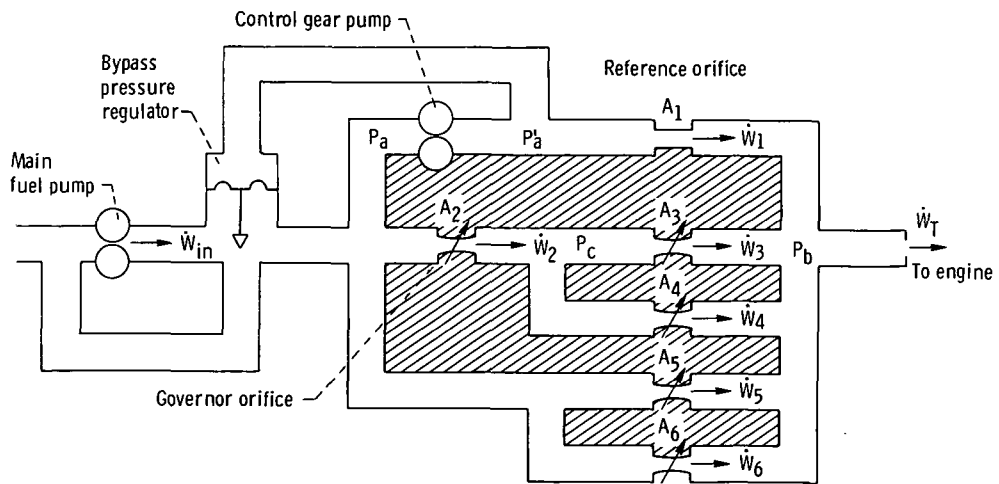


Figure 2. - Schematic of fuel control system.

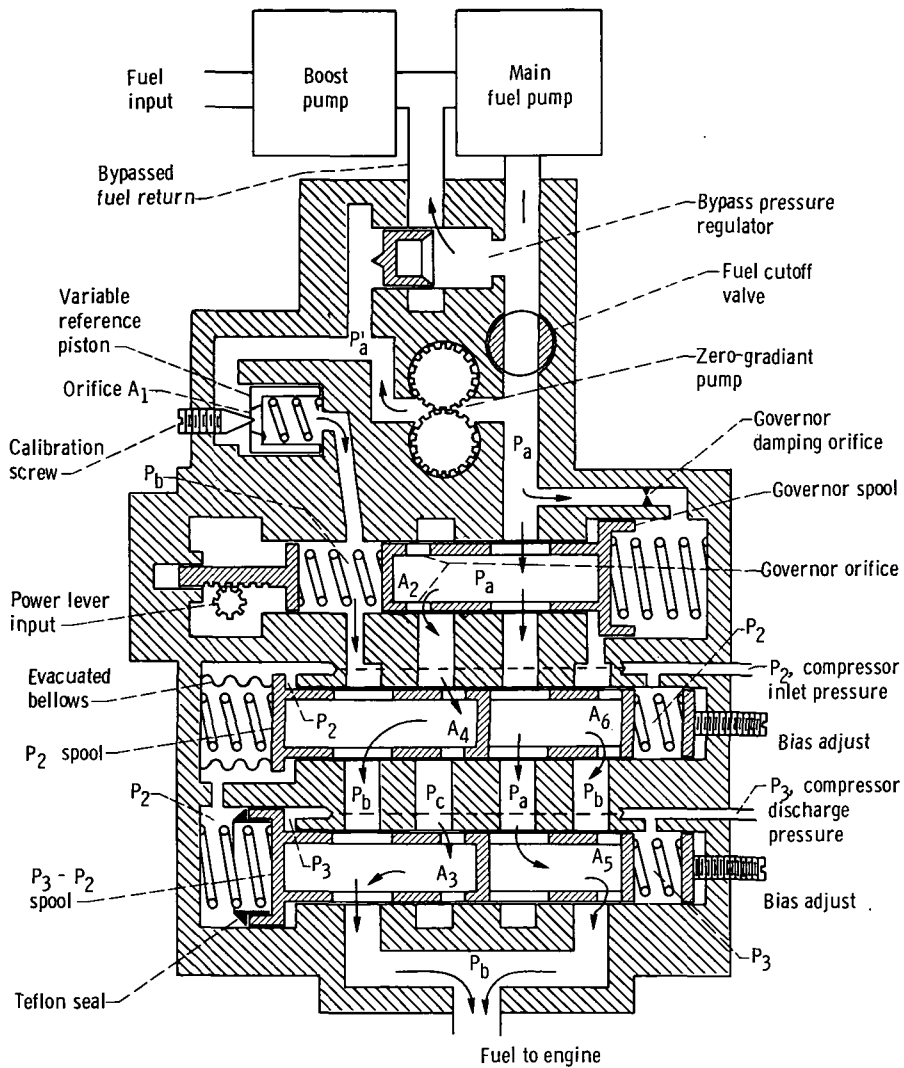


Figure 3. - Simplified cross-sectional view of generalized-parameter fuel control.

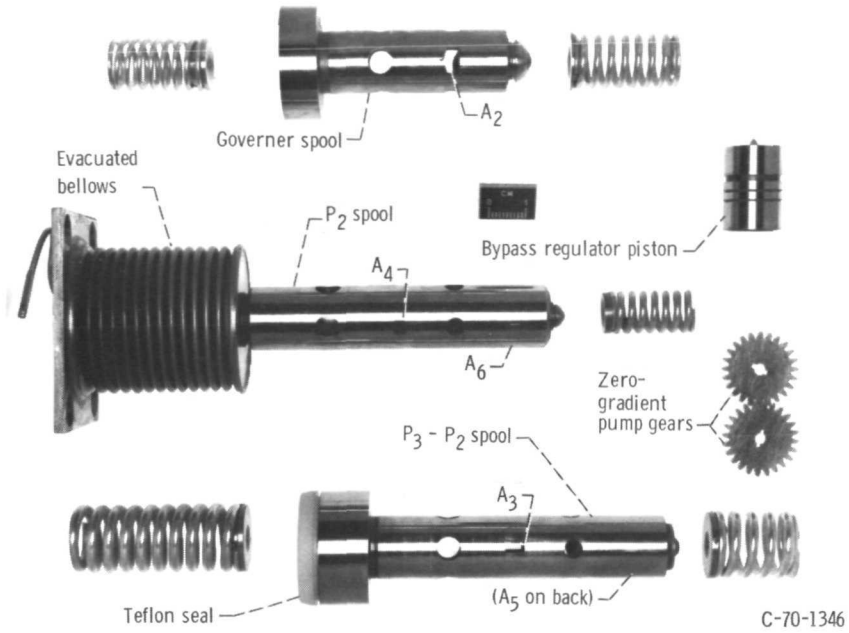


Figure 4. - Actual components used in generalized-parameter fuel control.

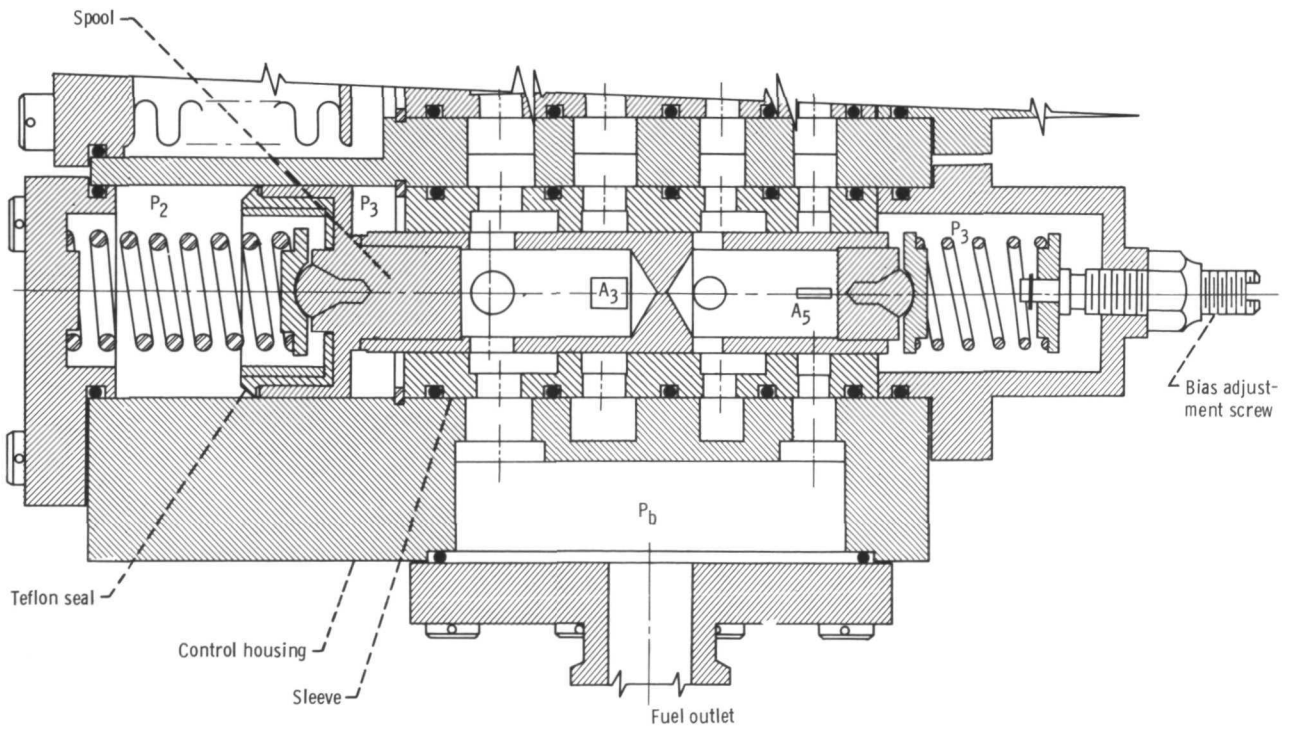


Figure 5. - Detailed cross-sectional view of  $P_3 - P_2$  spool.

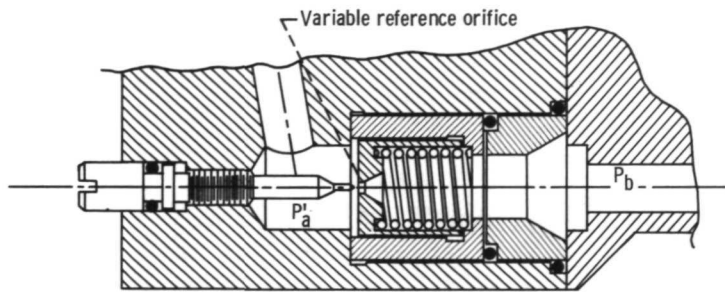


Figure 6. - Cross-sectional view of variable reference orifice.

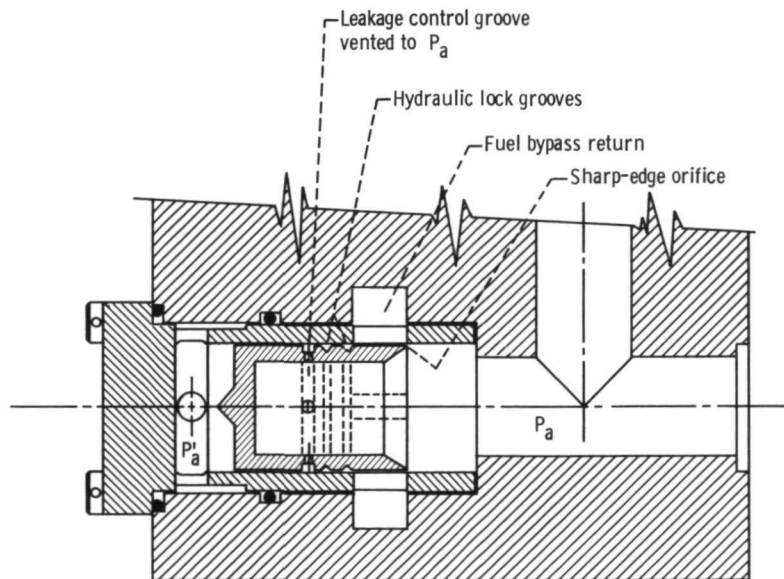


Figure 7. - Cross-sectional view of zero-gradient-pump bypass pressure regulator.

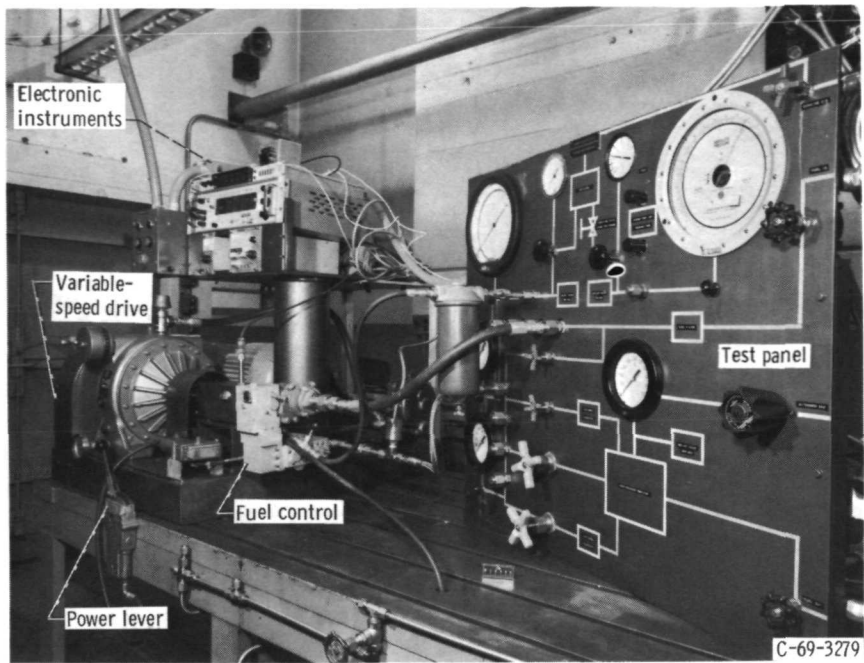


Figure 8. - Test bench.

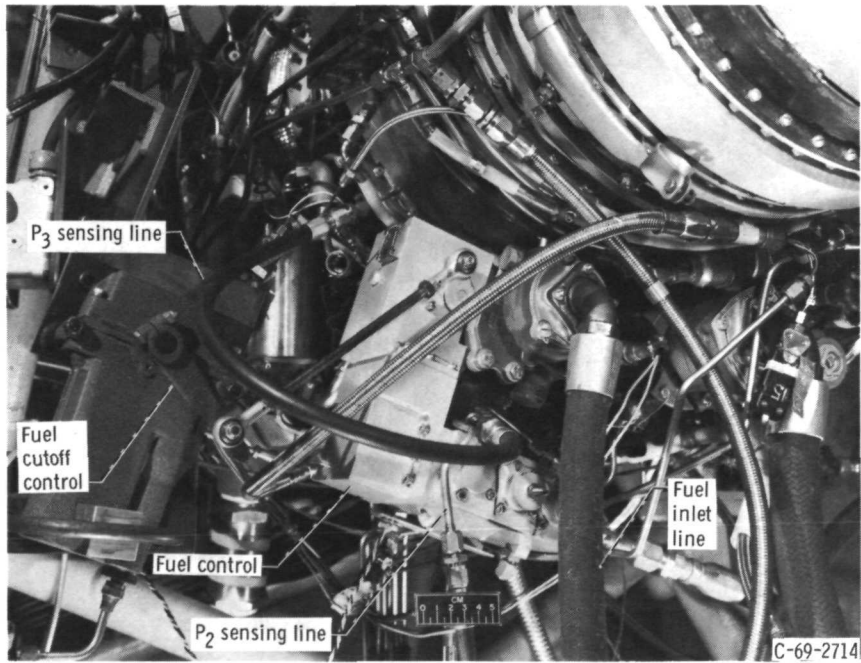


Figure 9. - Engine installation.

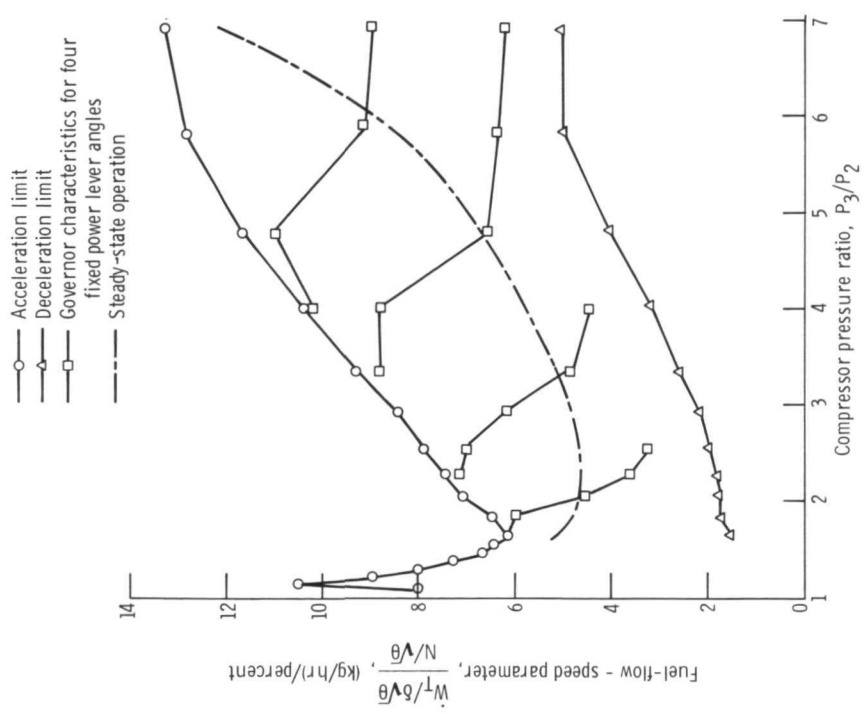


Figure 10. - Corrected parameter map of acceleration, deceleration, and selected governor characteristics for fuel control. Compressor face pressure  $P_2$ , 10 N/cm<sup>2</sup>; square-edge pressure regulator.

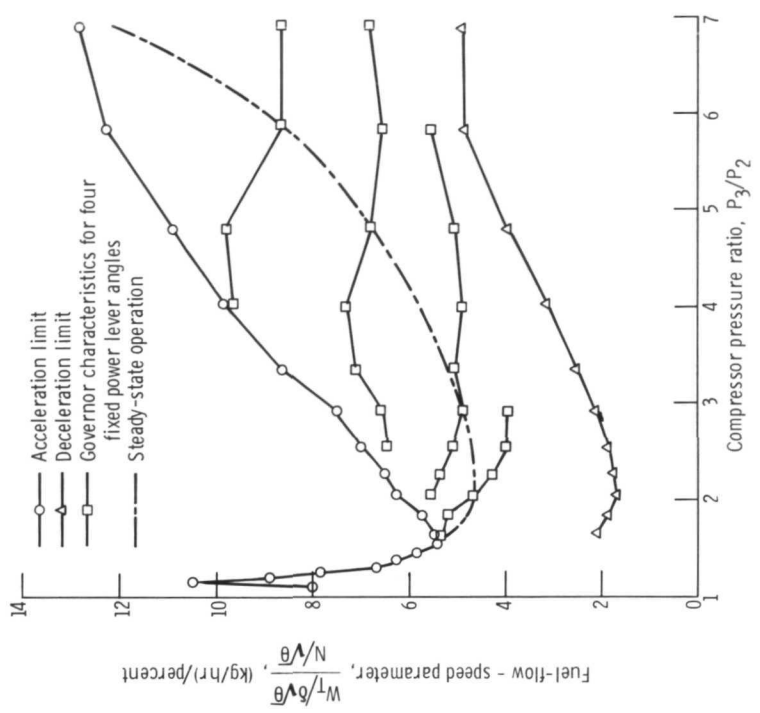


Figure 11. - Corrected parameter map of acceleration, deceleration, and selected governor characteristics for fuel control. Compressor face pressure  $P_2$ , 10 N/cm<sup>2</sup>; sharp-edge pressure regulator.

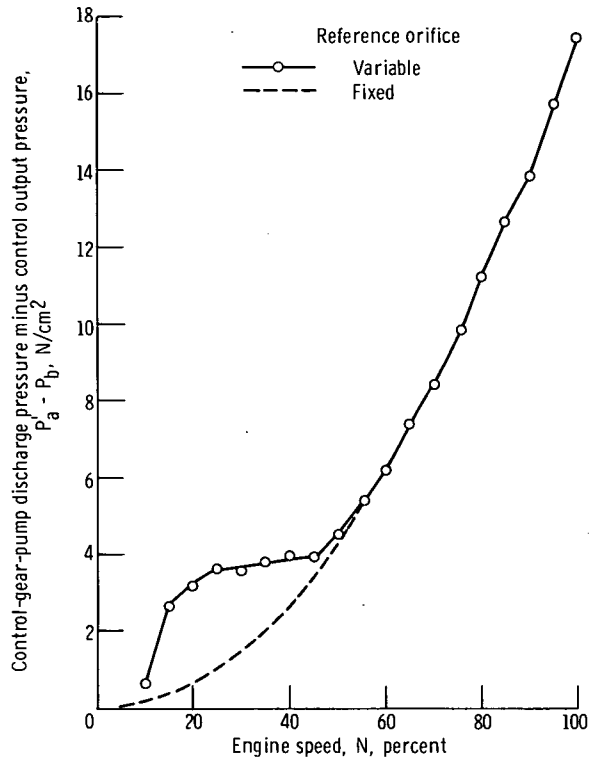


Figure 12. - Variable-reference-orifice pressure drop as function of control speed.

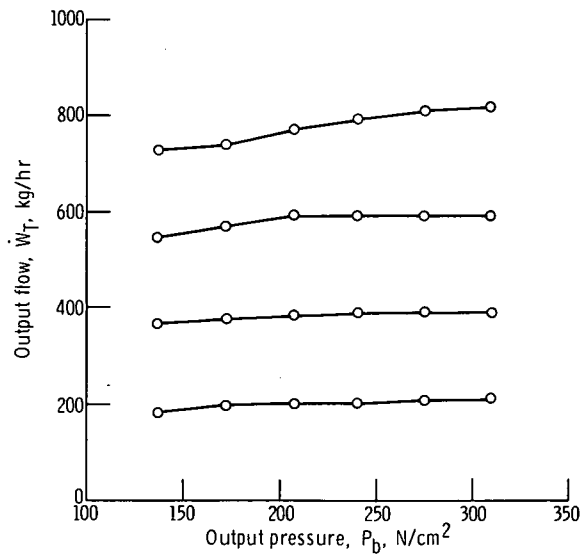


Figure 13. - Output flow-pressure characteristic at four control output flows.

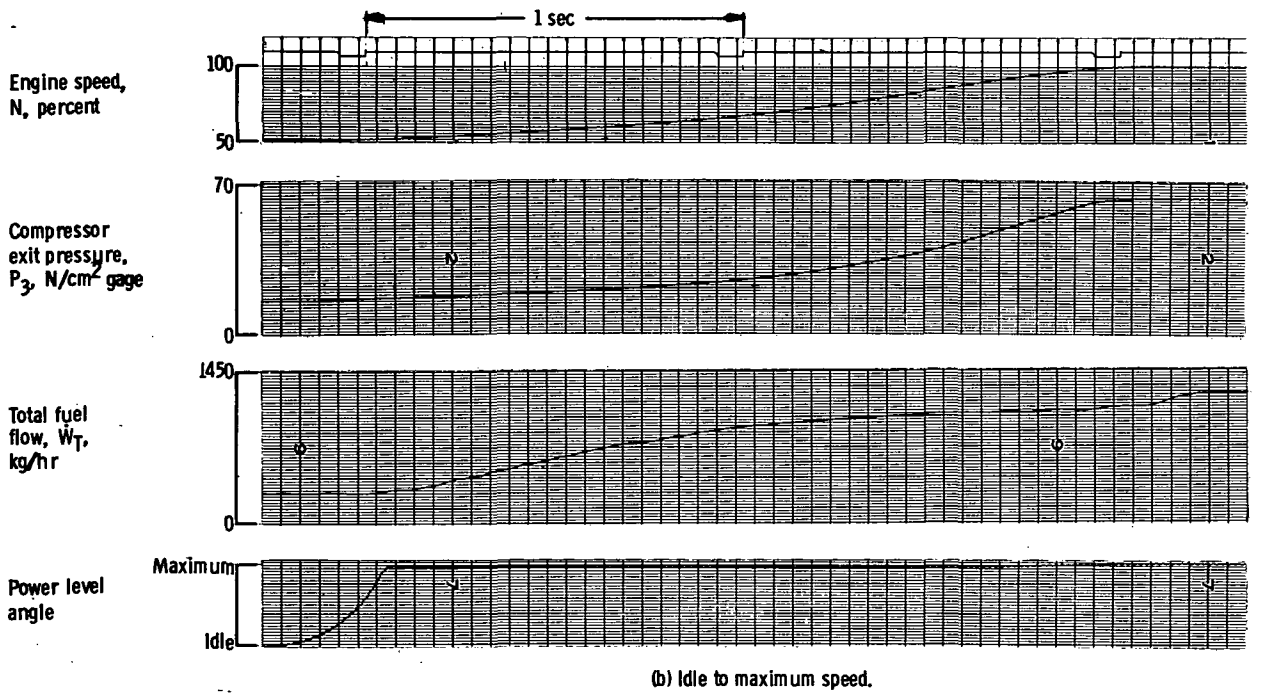
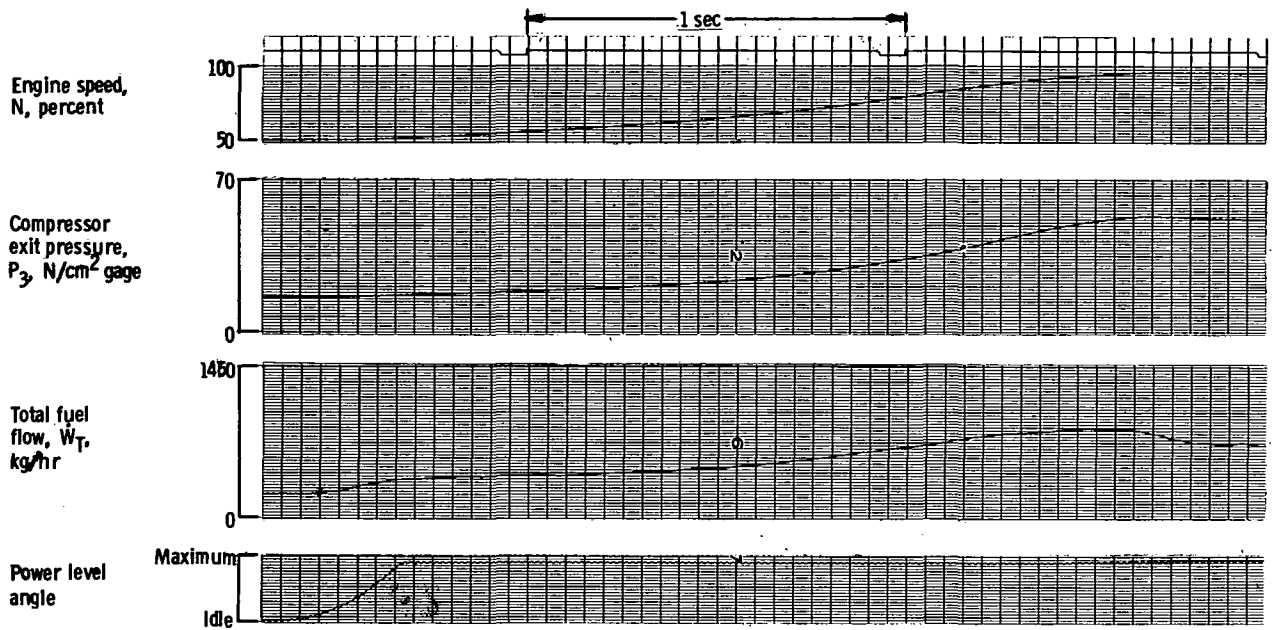
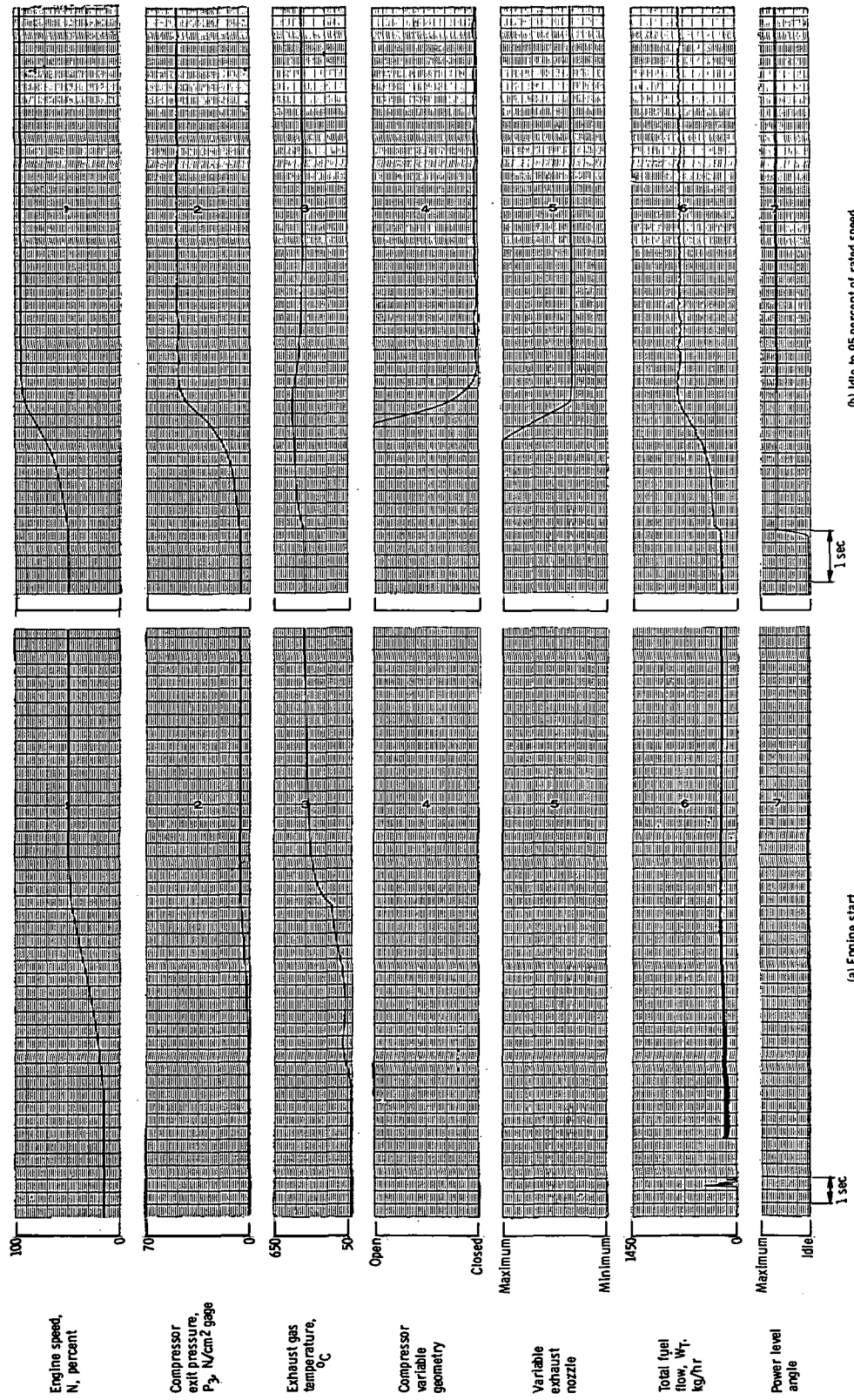
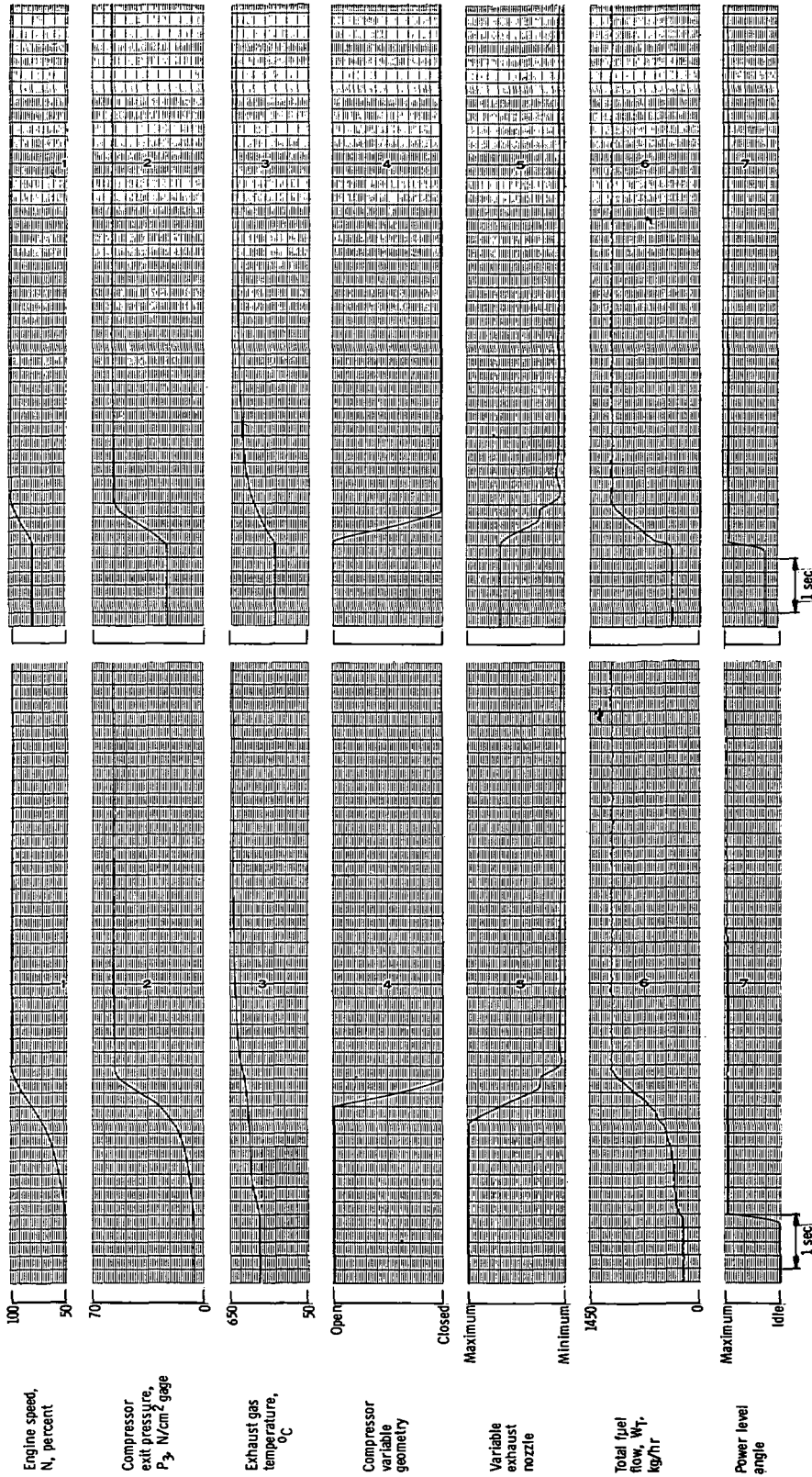


Figure 14. - Engine acceleration transients with control schedules as shown in figure 10.



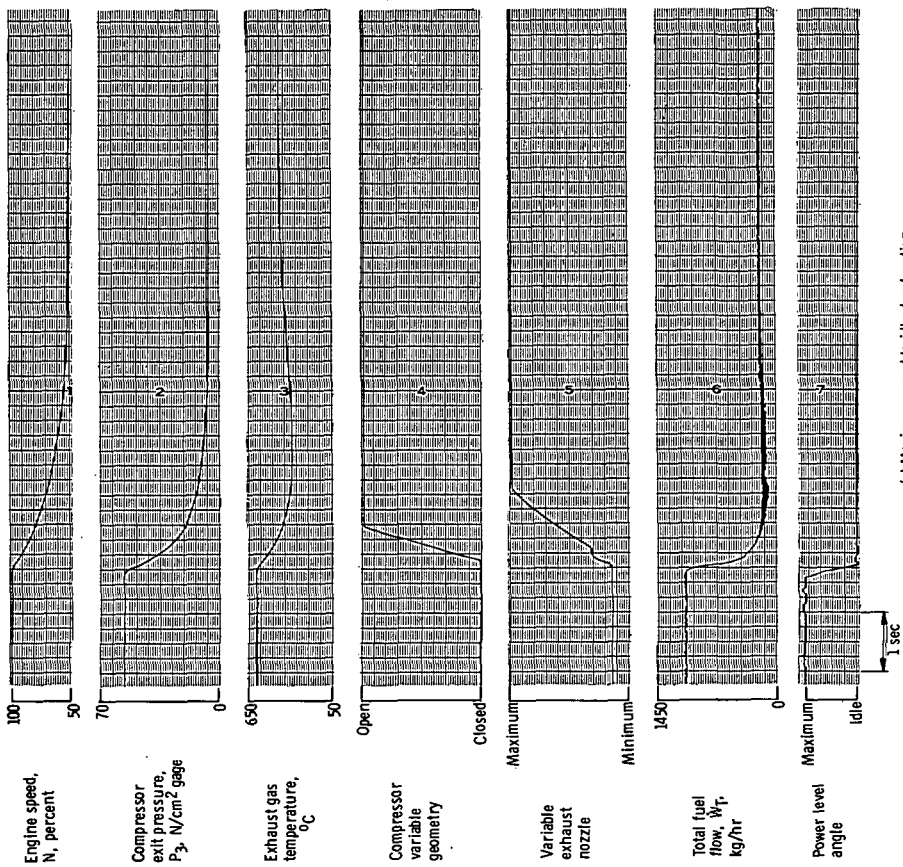
(a) Engine start. (b) Idle to 95 percent of rated speed. Figure 15. - Engine transients with control schedules as shown in figure 11.



(d) Eighty percent of rated speed to maximum speed.

(c) Idle to maximum speed.

Figure 15. - Continued.



(e) Maximum speed to idle deceleration.

Figure 15. - Concluded.

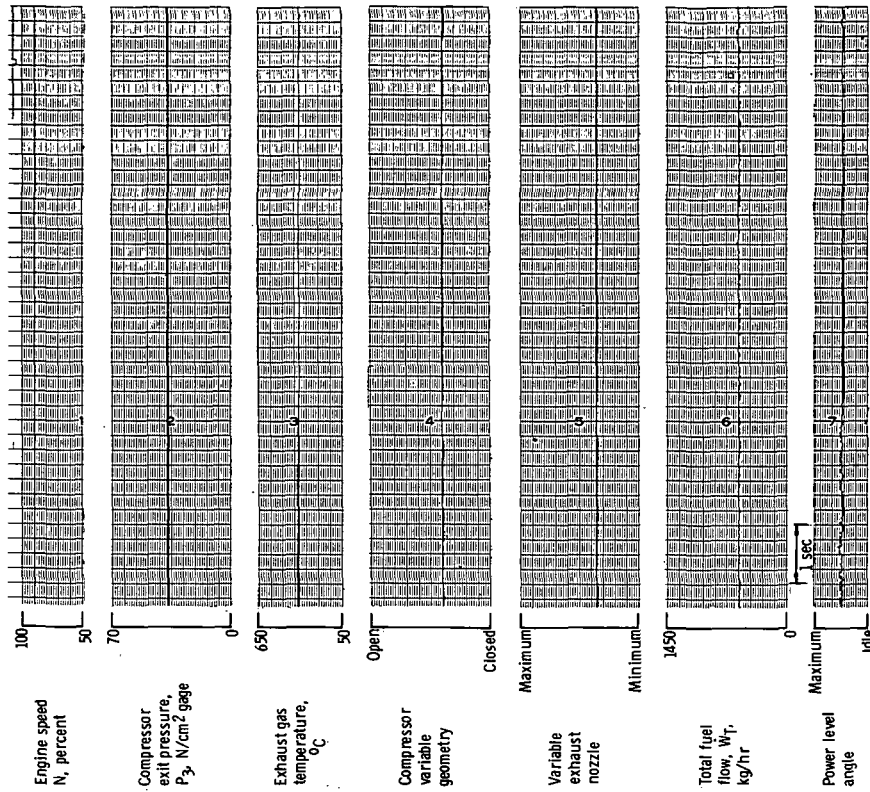


Figure 16. - Ninety-percent-rated-speed steady-state condition.



POSTMASTER: If Undeliverable (Section 158  
Postal Manual) Do Not Return

*"The aeronautical and space activities of the United States shall be conducted so as to contribute . . . to the expansion of human knowledge of phenomena in the atmosphere and space. The Administration shall provide for the widest practicable and appropriate dissemination of information concerning its activities and the results thereof."*

—NATIONAL AERONAUTICS AND SPACE ACT OF 1958

## NASA SCIENTIFIC AND TECHNICAL PUBLICATIONS

**TECHNICAL REPORTS:** Scientific and technical information considered important, complete, and a lasting contribution to existing knowledge.

**TECHNICAL NOTES:** Information less broad in scope but nevertheless of importance as a contribution to existing knowledge.

**TECHNICAL MEMORANDUMS:** Information receiving limited distribution because of preliminary data, security classification, or other reasons. Also includes conference proceedings with either limited or unlimited distribution.

**CONTRACTOR REPORTS:** Scientific and technical information generated under a NASA contract or grant and considered an important contribution to existing knowledge.

**TECHNICAL TRANSLATIONS:** Information published in a foreign language considered to merit NASA distribution in English.

**SPECIAL PUBLICATIONS:** Information derived from or of value to NASA activities. Publications include final reports of major projects, monographs, data compilations, handbooks, sourcebooks, and special bibliographies.

**TECHNOLOGY UTILIZATION PUBLICATIONS:** Information on technology used by NASA that may be of particular interest in commercial and other non-aerospace applications. Publications include Tech Briefs, Technology Utilization Reports and Technology Surveys.

*Details on the availability of these publications may be obtained from:*

**SCIENTIFIC AND TECHNICAL INFORMATION OFFICE**

**NATIONAL AERONAUTICS AND SPACE ADMINISTRATION**

**Washington, D.C. 20546**